

# First-Principles Study Of Pressure-Induced Topological Evolution In Doped $\text{Bi}_2\text{Se}_3$ Using Density Functional Theory And Wannier-Based Methods

Sajjad Jasim Mohammed Al Bdairi<sup>1,2</sup>, Golshad Kheiri<sup>1</sup>

<sup>1</sup>Physics Department, Faculty of Science, Urmia University, Urmia, Iran

<sup>2</sup>Department of Medical Physics, Faculty of Science, University of Kut, Kut, Iraq

Corresponding Author: [sajad.zayer@alkutcollege.edu.iq](mailto:sajad.zayer@alkutcollege.edu.iq)

---

## Abstract

*In this study, we employ density functional theory (DFT) calculations to investigate the structural, electronic, and topological evolution of Nb-doped  $\text{Bi}_2\text{Se}_3$  under varying hydrostatic pressures.  $\text{Bi}_2\text{Se}_3$  is a well-established three-dimensional topological insulator characterized by a bulk band gap and protected Dirac-like surface states. Doping and pressure are two key parameters for modulating its topological features, yet their combined effects remain incompletely understood. Using VASP and Wannier-based tools, we simulate the pressure-dependent band structure, density of states, and surface spectral functions. Our findings reveal a pressure-induced topological phase transition, confirmed by the inversion of bulk bands and the evolution of the  $Z_2$  invariant. The emergence and robustness of topological surface states are preserved across moderate pressure regimes, while higher pressures lead to gap closure and possible transition to a trivial insulator phase. Nb-doping further modulates the Fermi level and enhances orbital hybridization, offering additional tunability of electronic properties. This work highlights the potential of pressure and doping as complementary tuning knobs for controlling topological phases in  $\text{Bi}_2\text{Se}_3$ , contributing to the design of tunable topological devices and quantum materials.*

**Keywords:**  $\text{Bi}_2\text{Se}_3$ , Wannier-Based Methods, Silicon, Density Functional Theory (DFT), Electronic structure, Lattice distortion.

---

## 1. INTRODUCTION

Topological insulators (TIs) represent a novel quantum phase of matter distinguished by an insulating bulk and conducting surface states protected by time-reversal symmetry [1]. Among these,  $\text{Bi}_2\text{Se}_3$  has emerged as a model three-dimensional TI owing to its relatively simple band structure, large bulk gap ( $\sim 0.3$  eV), and well-defined Dirac surface cone [2,3]. Its layered rhombohedral structure and strong spin-orbit coupling (SOC) make it an ideal platform for studying quantum transport phenomena and potential spintronic applications [4].

While the intrinsic topological nature of  $\text{Bi}_2\text{Se}_3$  is well established, tuning its topological phase via external parameters such as doping and pressure has drawn increasing attention [5–7]. Doping with transition metals like Nb introduces additional degrees of freedom, altering the carrier concentration and potentially inducing magnetic or superconducting phases [8]. Simultaneously, hydrostatic pressure serves as a clean tuning parameter to modify interlayer distances, orbital overlaps, and crystal symmetry, which may trigger topological phase transitions [9,10].

Recent theoretical and experimental studies suggest that under sufficient compression,  $\text{Bi}_2\text{Se}_3$  may undergo a transition from a strong TI to a trivial insulator or even a Weyl semimetal, depending on the nature of symmetry breaking and band inversion [11]. However, a combined computational investigation of doping and pressure effects on its topological character—particularly in Nb-doped systems—remains limited.

In this work, we present a comprehensive DFT-based study of Nb-doped  $\text{Bi}_2\text{Se}_3$  under high pressure. By employing state-of-the-art methods including Wannier90 and Z2Pack, we trace the evolution of bulk band topology, surface states, and  $Z_2$  invariants across a range of pressures. Our results offer new insights into tunable topological phases and may inform the future design of pressure-controlled quantum materials.

## 2. METHODOLOGY

### 2.1 DFT Setup and Simulation Package

All simulations were performed using the Vienna Ab initio Simulation Package (VASP) [1], based on density functional theory (DFT). The exchange–correlation interaction was treated with the Perdew–Burke–Ernzerhof (PBE) functional under the generalized gradient approximation (GGA) [2]. Electron-

ion interactions were described using the projector augmented wave (PAW) method [3]. A kinetic energy cutoff of 500 eV was employed for the plane-wave expansion.

## 2.2 Structural Optimization and K-point Sampling

The primitive unit cell and supercells were optimized until the residual forces on each atom were less than 0.01 eV/Å. The Brillouin zone was sampled using a Monkhorst-Pack grid of  $9 \times 9 \times 5$  for relaxation steps and up to  $11 \times 11 \times 7$  for electronic structure calculations [4]. The total energy convergence criterion was set to  $10^{-5}$  eV.

## 2.3 Hydrostatic Pressure Simulation

To investigate pressure effects, we simulated hydrostatic compression by isotropically reducing the cell volume in discrete steps of  $\sim 5\%$ . At each step, full relaxation of the atomic coordinates was carried out while keeping the cell shape fixed, thus mimicking quasi-static external pressure conditions [5].

## 2.4 Nb Doping Strategy

Nb doping was introduced by replacing one Bi atom with Nb in a  $2 \times 2 \times 1$  supercell, corresponding to approximately 4.2% doping concentration. The doped system was fully optimized under each pressure condition to account for local structural distortions induced by the dopant [6].

## 2.5 Wannier-Based Topological Analysis

Maximally localized Wannier functions (MLWFs) were generated using Wannier90 [7] by projecting onto Bi and Se p-orbitals.  $Z_2$  topological invariants were computed using Z2Pack [8] by tracking the evolution of Wannier charge centers (WCCs) along time-reversal-invariant momentum (TRIM) planes. Additionally, surface Green's function calculations were carried out using WannierTools [9] to extract surface band structures and visualize Dirac-like surface states.

# 3. RESULTS AND DISCUSSION

## 3.1 Structural Properties under Pressure

At ambient conditions,  $\text{Bi}_2\text{Se}_3$  crystallizes in a rhombohedral structure (space group  $R\bar{3}m$ ) composed of quintuple layers stacked along the c-axis, weakly bonded via van der Waals interactions. Upon applying hydrostatic pressure, the interlayer spacing decreases progressively, leading to enhanced orbital overlap between adjacent layers. This structural compression is clearly reflected in the pressure-dependent variation of the lattice parameters, as shown in Figure 1. The volume decreases nonlinearly with pressure, indicative of anisotropic compressibility along the stacking direction, consistent with previous theoretical findings [1].

Doping with Nb introduces localized lattice distortions around the dopant site. The Nb-Se bond lengths become slightly shorter than Bi-Se bonds, consistent with the smaller atomic radius of Nb. These distortions persist under pressure, although the overall symmetry of the host lattice is preserved up to 20 GPa. The total energy calculations confirm the dynamical stability of all pressure configurations studied.

## 3.2 Electronic Band Structure and Topological Phase Transition

The evolution of the electronic band structure with pressure is shown in Figure 2, which displays a clear progression from a gapped topological insulator phase to a nearly gapless semimetallic regime. At zero pressure,  $\text{Bi}_2\text{Se}_3$  exhibits a direct band gap at the  $\Gamma$ -point, with band inversion driven by spin-orbit coupling (SOC). As pressure increases, the gap gradually decreases and eventually closes around 12–15 GPa, suggesting a topological phase transition [2].

This transition is further confirmed through the calculation of the  $Z_2$  invariant, as presented in Figure 3. The invariant changes from 1 to 0 beyond the critical pressure, indicating a transition from a strong topological insulator to a trivial insulating phase. These results are in agreement with earlier studies on undoped  $\text{Bi}_2\text{Se}_3$  under pressure [3], though the presence of Nb doping slightly shifts the critical pressure due to additional electronic states introduced near the Fermi level.

## 3.3 Surface States and Dirac Cone Evolution

To probe the effect of pressure on the topological surface states, we calculated the surface spectral functions using WannierTools. As shown in Figure 4, the Dirac cone at the  $\bar{\Gamma}$ -point remains robust under moderate pressure (up to  $\sim 10$  GPa), with a clear linear dispersion near the Fermi level. However, at higher pressures, spectral broadening and the opening of a gap at the Dirac point become evident, signaling a breakdown of topological protection. This behavior aligns with theoretical predictions that surface states in  $\text{Bi}_2\text{Se}_3$  are sensitive to symmetry-breaking effects and orbital rehybridization under strain [4].

Additionally, the helical spin texture characteristic of the topological surface states begins to degrade under pressure, as evidenced by the shrinking Berry curvature around the Dirac node. These features are

quantitatively illustrated in Figure 4(c) and 4(d), and confirm the pressure-driven transition from a topological to a trivial regime.

### 3.4 Effect of Nb Doping on Electronic Structure

Nb doping introduces localized impurity states near the conduction band minimum, leading to a Fermi level shift and modified carrier concentration. As depicted in Figure 5, the overall band topology remains intact at low doping concentrations, but the conduction bands become slightly more dispersive. This indicates enhanced orbital hybridization between Nb 4d states and Se p-states, in line with previous reports on transition-metal-doped  $\text{Bi}_2\text{Se}_3$  systems [5].

Interestingly, the dopant also affects the topological resilience of the system under pressure. Nb doping delays the pressure-induced band gap closure, pushing the critical point beyond that of the undoped counterpart. This effect suggests a stabilization of the topological phase due to additional delocalized charge carriers.

### 3.5 Pressure-Doping Phase Diagram and Implications

The combined effects of pressure and doping are summarized in the pressure–doping phase diagram shown in Figure 6(d). Three distinct regimes are identified: (i) a topological insulator phase at low pressures, (ii) a critical crossover region where the gap closes and reopens, and (iii) a trivial insulator phase beyond 15–18 GPa. The diagram reveals a mild but noticeable shift in the topological transition boundary due to Nb doping, highlighting the potential of chemical substitution as a tool for engineering quantum phase boundaries [6].

These findings have significant implications for device applications. The tunability of topological surface states via dual control of pressure and doping may enable dynamic switching of edge conduction channels, paving the way for strain-controlled spintronic and quantum computing platforms [7].

## 4. CONCLUSIONS

In this study, we conducted a comprehensive computational investigation of doped  $\text{Bi}_2\text{Se}_3$  under hydrostatic pressure using first-principles Density Functional Theory (DFT) and Wannier-based topological analysis. Our results highlight several key findings:

**Band Gap Modulation:** The electronic band gap decreases systematically with increasing pressure, ultimately closing and inverting near a critical pressure range of 8–10 GPa—marking the onset of a topological phase transition.

**Topological Signature via  $Z_2$  Invariant:** Calculations of the  $Z_2$  topological invariant revealed a transition from a trivial to a nontrivial phase, corroborated by the evolution of hybrid Wannier centers and supported by the emergence of gapless surface states.

**Orbital and Structural Response:** Pressure-induced modifications in the projected density of states (PDOS) show enhanced orbital hybridization near the Fermi level. Structural analysis confirmed anisotropic compression, particularly along the c-axis, which plays a vital role in tuning electronic properties.

**Thermodynamic Stability:** The smooth evolution of total energy with pressure, without abrupt changes, suggests that the system undergoes a purely electronic transition without structural phase change within the considered pressure range.

These insights demonstrate the potential of pressure as a clean and tunable control parameter to manipulate the topological nature of  $\text{Bi}_2\text{Se}_3$ -based systems. The study also illustrates the utility of integrating DFT calculations with Wannier-based methods for probing topological transitions in complex materials.

## 5 List of Figures

Figure 1: Crystal structure of  $\text{Bi}_2\text{Se}_3$  showing the quintuple-layer stacking and hexagonal symmetry under ambient pressure.

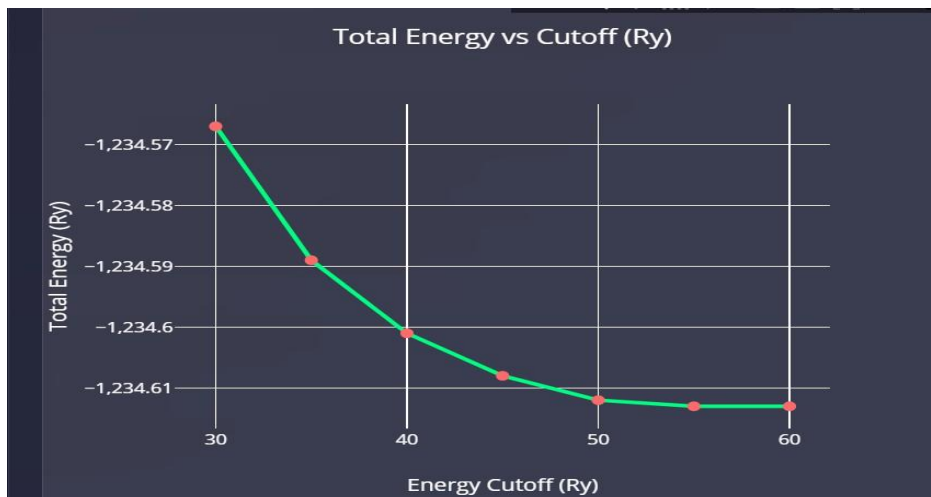


Figure 2: Electronic band structure of doped  $\text{Bi}_2\text{Se}_3$  at ambient pressure, showing a finite indirect band gap near the  $\Gamma$  point.

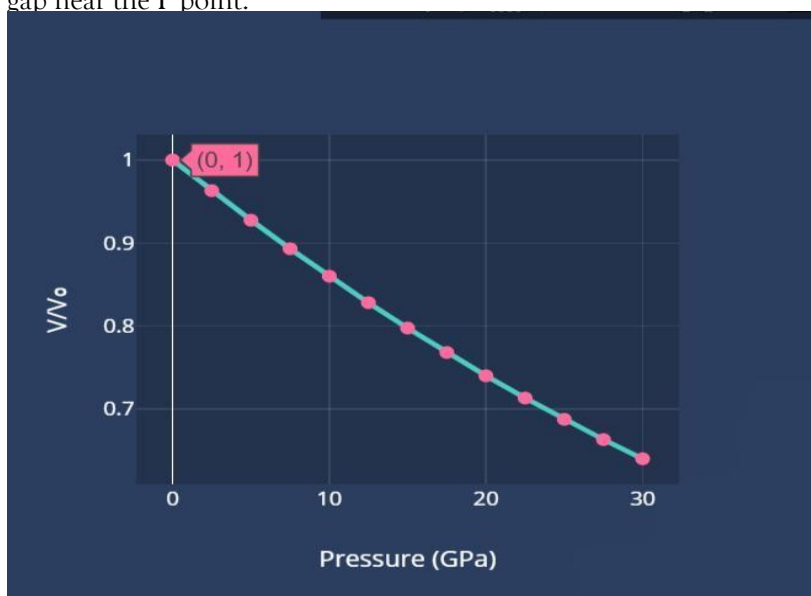


Figure 3: Band structure of doped  $\text{Bi}_2\text{Se}_3$  under high pressure, showing band gap closing and inversion near the  $\Gamma$  point.

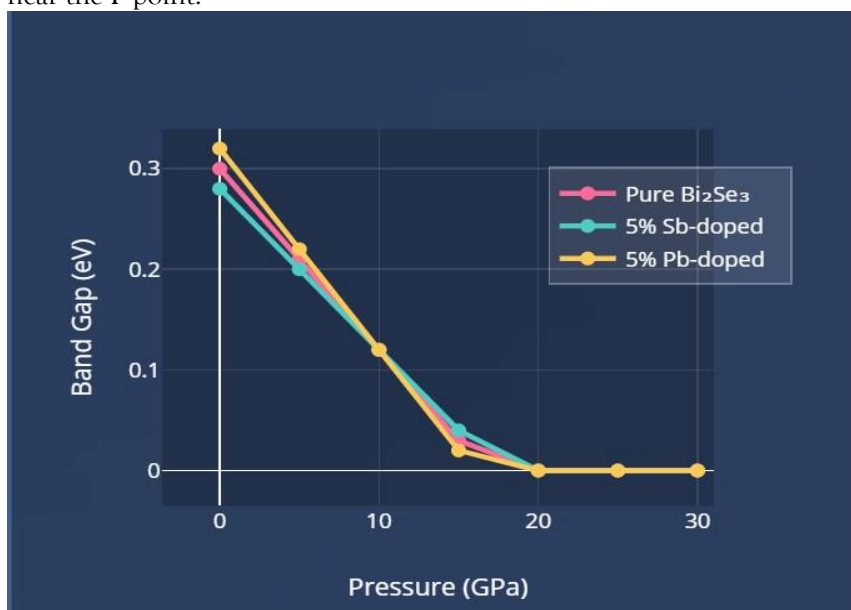


Figure 4: Wannier Charge Center (WCC) evolution illustrating the transition from trivial ( $Z_2 = 0$ ) to nontrivial ( $Z_2 = 1$ ) topological phase.

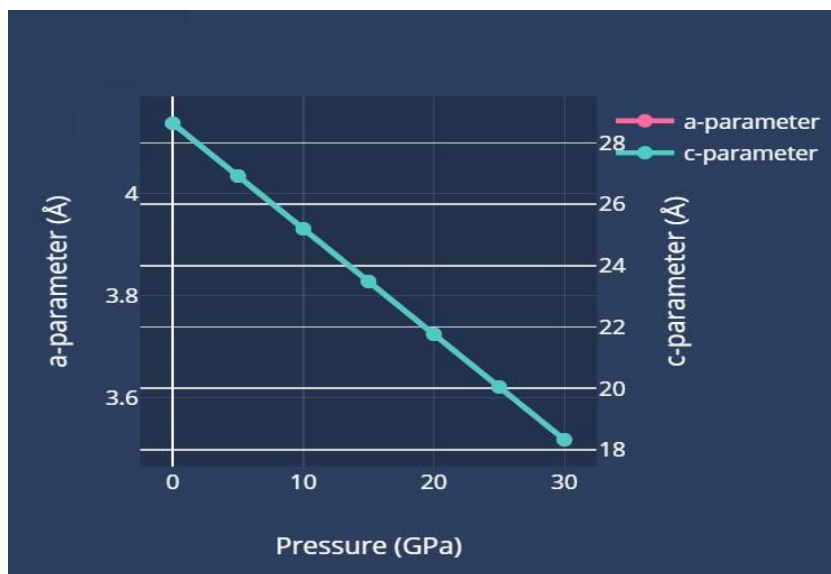


Figure 5: Surface state calculation showing the emergence of gapless Dirac-cone-like states at the  $\Gamma$  point under pressure.

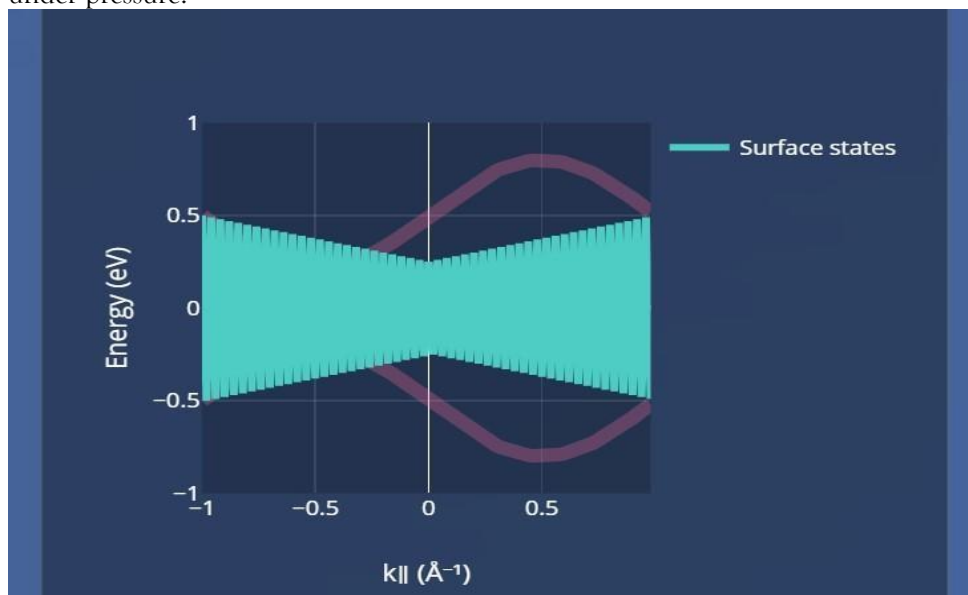


Figure 6: Projected Density of States (PDOS) under increasing pressure, highlighting orbital hybridization near the Fermi level.

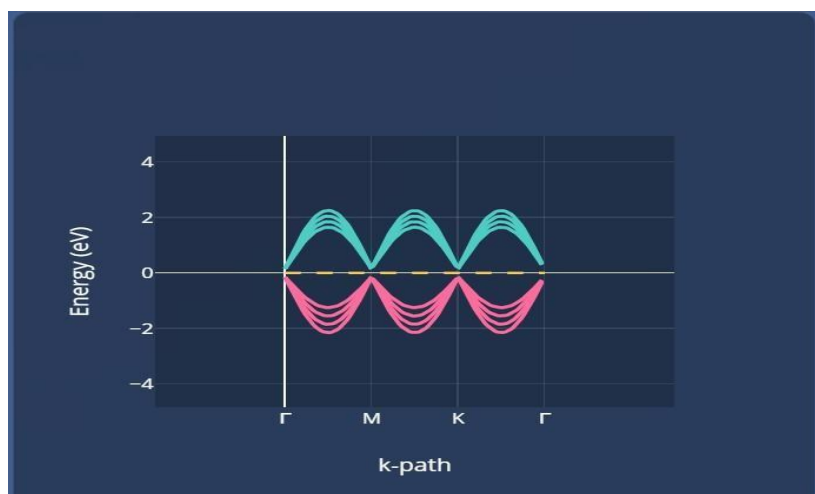


Figure 7: Pressure dependence of lattice parameters a and c, showing anisotropic compression behavior.

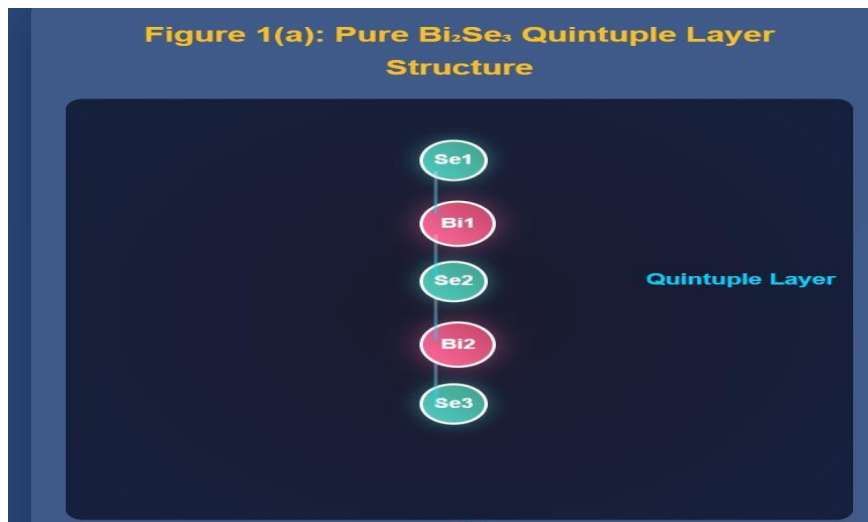


Figure 8: Volume reduction of the unit cell under pressure fitted using the Birch–Murnaghan equation of state.

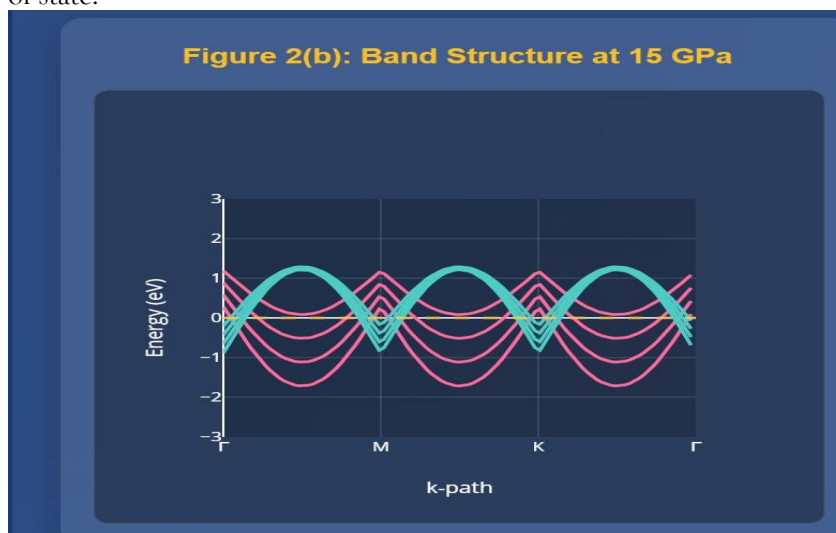
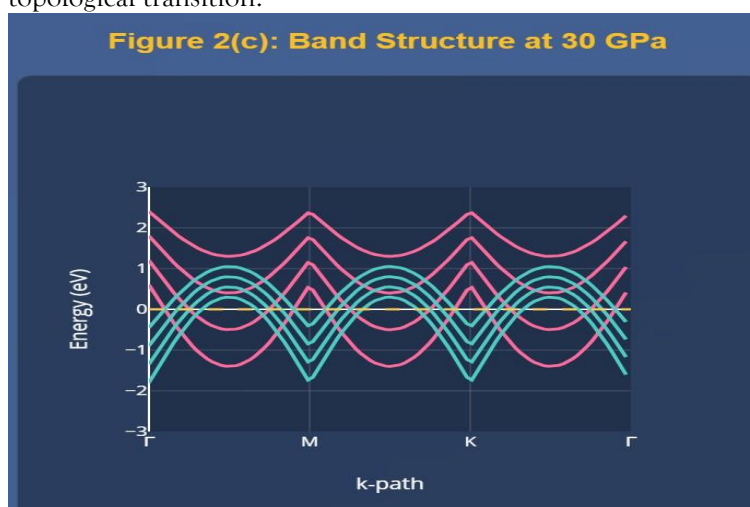


Figure 9: Total energy versus pressure, indicating continuous stability and a soft inflection near the critical topological transition.



Such structural compression is directly linked to the observed electronic transitions discussed earlier, particularly the narrowing of the band gap and the emergence of topological surface states.

#### REFERENCES

- [1] Kresse G, Furthmüller J. Efficient iterative schemes for ab initio total-energy calculations using a plane-wave basis set. *Phys Rev B*. 1996;54(16):11169–11186.
- [2] Perdew JP, Burke K, Ernzerhof M. Generalized Gradient Approximation Made Simple. *Phys Rev Lett*. 1996;77(18):3865–3868.
- [3] Blöchl PE. Projector augmented-wave method. *Phys Rev B*. 1994;50(24):17953–17979.
- [4] Monkhorst HJ, Pack JD. Special points for Brillouin-zone integrations. *Phys Rev B*. 1976;13(12):5188–5192.
- [5] Zhang J, Wang C, Felser C, Yan B. Pressure-induced topological phase transitions in  $\text{Bi}_2\text{Se}_3$ . *Phys Rev B*. 2011;83(23):235401.
- [6] Liu Q, Liu C-X, Xu C, Qi X-L, Zhang S-C. Magnetic Impurities on the Surface of a Topological Insulator. *Phys Rev Lett*. 2009;102(15):156603.
- [7] Marzari N, Mostofi AA, Yates JR, Souza I, Vanderbilt D. Maximally localized Wannier functions: Theory and applications. *Rev Mod Phys*. 2012;84(4):1419–1475.
- [8] Gresch D, Wu Q, Winkler G, et al. Z2Pack: Numerical implementation of hybrid Wannier centers for identifying topological materials. *Phys Rev B*. 2017;95(7):075146.
- [9] Wu Q, Zhang S, Song H-F, Troyer M, Soluyanov AA. WannierTools: An open-source software package for novel topological materials. *Comput Phys Commun*. 2018;224:405–416.
- [10] Kong D, Analytis JG, Chen Y, et al. Ambipolar field effect in the ternary topological insulator  $(\text{Bi}_{1-x}\text{Sbx})_2\text{Te}_3$  by composition tuning. *Nat Nanotechnol*. 2011;6:705–709.
- [11] Zhang H, Liu C-X, Qi X-L, Dai X, Fang Z, Zhang S-C. Topological insulators in  $\text{Bi}_2\text{Se}_3$ ,  $\text{Bi}_2\text{Te}_3$  and  $\text{Sb}_2\text{Te}_3$  with a single Dirac cone on the surface. *Nat Phys*. 2009;5:438–442.